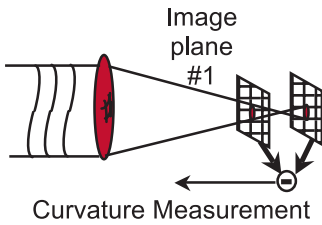


## Curvature Wavefront Sensor and Error

---



curvature term minus the derivative of the wavefront at the edge  $\frac{d\Phi(\mathbf{r})}{d\mathbf{n}}$ :

$$I_1(\mathbf{r}) - I_2(\mathbf{r}) = C \left[ \nabla^2 \Phi(\mathbf{r}) - \frac{d\Phi(\mathbf{r})}{d\mathbf{n}} \right]$$

To provide an accurate measurement of wavefront curvature, the **blur** from the turbulence must be small compared to the area where the curvature measurement is taken. With  $p$  being the offset from the focal plane of the system and  $f$  as the focal length of the system, a conservative estimate of the blur requirement leads to

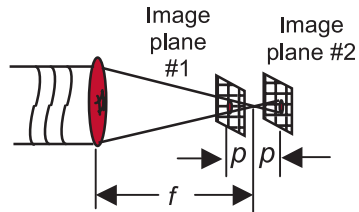
$$p \geq \frac{\lambda f^2}{\lambda f + r_0^2}$$

**Variance of a single curvature measurement:**

$$\sigma_{\text{Curv. Sens.}}^2 = \frac{p^2}{f^4 N_p}$$

where  $N_p$  is the photon count. Because the curvature sensor directly measures the Laplacian of the wavefront, **bimorph mirrors** are generally used for closed-loop compensation, as they possess Laplacian influence functions.

The **curvature sensor** is an image-plane measurement of local wavefront curvature [the second **derivative** of the wavefront  $\nabla^2 \Phi(\mathbf{r})$ ] deduced from two specific out-of-focus images. A point-by-point subtraction of the images is proportional to the wavefront curvature term minus the



## Pyramid Wavefront Sensor and Error

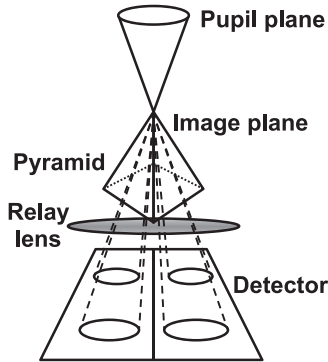
The **pyramid wavefront sensor** is a pupil-plane wavefront sensor.

Another pupil-plane wavefront sensor uses a pyramidal prism in the image plane to create four subbeams that are then optically relayed to a detector. The intensity at position  $\vec{r}(x, y)$  in each of the subbeams in the detector plane ( $I_{0,0} > I_{0,1} > I_{1,0} > I_{1,1}$ ) is used to find the  $x$  and  $y$  wavefront slopes at  $\vec{r}(x, y)$ :

$$S_x(\vec{r}) = \frac{I_{0,0}(\vec{r}) - I_{1,0}(\vec{r}) + I_{0,1}(\vec{r}) - I_{1,1}(\vec{r})}{I_t} \quad \text{and}$$

$$S_y(\vec{r}) = \frac{I_{0,0}(\vec{r}) + I_{1,0}(\vec{r}) - I_{0,1}(\vec{r}) - I_{1,1}(\vec{r})}{I_t}$$

$I_t$  is the average intensity over the detector plane.



One advantage of the pyramid technique over a Shack–Hartmann sensor is that the spatial resolution of the sensor is the size of the detector pixel in contrast to the larger lenslet subaperture size of the Shack–Hartmann. The wavefront error variance associated with the pyramid technique is approximated by

$$\sigma^2 = \frac{1}{2N} + \frac{2(e_n)^2}{N} \quad \text{rad}^2$$

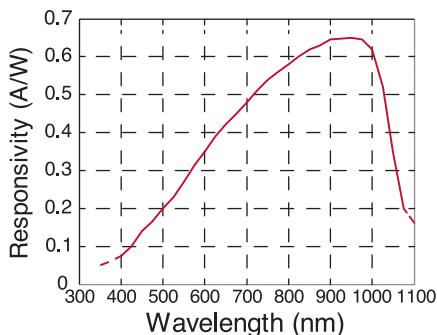
where  $N$  is the number of photons per pixel and  $e_n$  are the read-noise electrons.

## Photodiodes

**Photodiodes** are p–n junctions and have a **response time** that is a combination of drift time, diffusion time and resistor–capacitor (RC) time. The drift time is the time required to collect carriers in the depletion region, the diffusion time is the time required for collection of carriers in the undepleted bulk region, and the RC time is the response time due to the equivalent RC circuit.

Photodiodes can be operated in either photovoltaic or photoconductive mode. The photovoltaic mode has low noise, as it uses a zero-volt bias, which does not induce a dark current. Its response time is dominated by the drift time, as the carriers are not excited by a bias voltage. This mode is used for extremely low light level and low-frequency applications. The photoconductive mode uses a reverse bias voltage that increases the width of the depletion region and decreases the junction capacitance, increasing the response speed and linearity. This mode has a constant dark current and increased noise, and its response time is dominated by the diffusion time, as the carriers in the undepleted region have farther to travel.

The **responsivity**  $R$  of a photodiode is the ratio of the photocurrent to the incident power and is shown below for silicon. InGaAs is generally used for IR wavelengths.



## Photodiode Noise

**Photodiode noise** comes from **shot noise** and **Johnson noise**. Shot noise depends on the variance of the photocurrent and dark current:

$$I_s = \sqrt{2q(I_p + I_d)f}$$

Here  $q$  is the electron charge ( $1.6 \times 10^{-19}$  C),  $I_p$  is the photocurrent,  $I_d$  is the dark current, and  $f$  is the noise measurement bandwidth. Shot noise dominates when the photodiode is operated in photoconductive mode.

Johnson noise is generated by thermal carriers and is given as

$$I_J = \sqrt{\frac{4k_B T_K f}{R_p}}$$

Here  $k_B$  is the Boltzmann constant ( $1.38 \times 10^{-23}$  J/K),  $T_K$  is the temperature in Kelvin, and  $R_p$  is the parallel or shunt resistance. Johnson noise dominates when the photodiode is operated in photovoltaic mode, as this mode has no dark current and therefore very low shot noise.

The total noise current  $I_n$  is the root-sum-square (RSS) of the noise sources:

$$I_n = \sqrt{I_s^2 + I_J^2}$$

Johnson and shot noise are both white noise processes; however,  $1/f$  noise is also present where the power spectrum is inversely proportional to the frequency.  $1/f$  noise is commonly referred to as pink or flicker noise and has negligible magnitude for frequencies above 1 Hz, so it is typically ignored for noise performance analysis. This type of noise has been widely observed in many dynamic systems, and there is currently no universal theory for its origin.

**Noise equivalent power (NEP)** is the ratio of the total noise current to the responsivity and represents the level of incident intensity that generates a photocurrent equal to the noise current:

$$\text{NEP} = \frac{I_n}{R}$$